DENTAL MATERIALS 27 (2011) e87–e98

available at www.sciencedirect.com

ScienceDirect

journal homepage: www.intl.elsevierhealth.com/journals/dema

Identification of glutathione-methacrylates adducts in gingival fibroblasts and erythrocytes by HPLC–MS and capillary electrophoresis☆

Giuseppina Nocca[a,*], *Rino Ragno*[b], *Virginia Carbone*[c], *Giuseppe E. Martorana*[a], *Diana V. Rossetti*[a], *Gianluca Gambarini*[d], *Bruno Giardina*[a,e], *Alessandro Lupi*[e]

[a] *Institute of Biochemistry and Clinical Biochemistry, Catholic University, Rome, Italy*
[b] *Dipartimento di Chimica e Tecnologie del Farmaco dell'Università La Sapienza, Rome, Italy*
[c] *Istituto di Scienze dell' Alimentazione, CNR, Avellino, Italy*
[d] *Department of Dental Science, Sapienza University of Rome, Rome, Italy*
[e] *Istituto di Chimica del Riconoscimento Molecolare, CNR, Rome, Italy*

ARTICLE INFO

Article history:
Received 13 January 2010
Received in revised form
7 December 2010
Accepted 24 January 2011

Keywords:
Methacrylic monomers
GSH
Metabolism
HPLC–MS
Capillary electrophoresis

ABSTRACT

Objectives. Methacrylic monomers are released, from dental composite resins, either into the oral cavity or in pulpal tissues, where they can cause local or systemic adverse effects. The mechanisms of these effects are not well understood, probably because such molecules can act at different levels also inducing a depletion of intracellular glutathione (GSH). GSH can detoxify methacrylates by conjugating their α,β-unsaturated carbon–carbon moiety to the thiol group, with the catalysis of glutathione S-transferases (GST). This reaction determines a GSH cellular depletion and belongs to the metabolism of α,β-unsaturated esters, protecting the body against the toxic effects of electrophiles. On the basis of the above considerations, this work aim is to set up a method for the detection of the adducts formed by methacrylic monomers with GSH in cells using HPLC coupled to mass spectrometry (HPLC–MS) and micellar electrokinetic capillary chromatography (MECK) techniques.

Methods and results. Adducts of glutathione with triethylene glycol dimethacrylate (TEGDMA) and hydroxyethyl methacrylate (HEMA) were incontrovertibly identified by HPLC–MS and MECK in human gingival fibroblasts and erythrocytes, both outside and inside cells. Molecular docking simulations of HEMA and TEGDMA in the experimental structure of glutathione S-transferase, are also reported to rationalize the effectiveness of such enzyme in the catalysis of the above described reaction.

Significance. The setup of a method for the identification of GSH-methacrylate adducts allows to determine when the metabolic pathway involving such compounds is employed by cells for the detoxification of monomers leached from composite resins.

☆ GSH-methacrylates adducts in gingival fibroblasts.

* *Corresponding author at*: Institute of Biochemistry and Clinical Biochemistry, Catholic University, Largo Francesco Vito, 1, 00168 Rome, Italy. Tel.: +39 06 30154215; fax: +39 06 3053598.
E-mail address: g.nocca@rm.unicatt.it (G. Nocca).

0109-5641/$ – see front matter © 2011 Academy of Dental Materials. Published by Elsevier Ltd. All rights reserved.
doi:10.1016/j.dental.2011.01.002

1. Introduction

Methacrylic compounds – like triethylene glycol dimethacrylate (TEGDMA) and hydroxyethyl methacrylate (HEMA) – are used as components of polymeric materials commonly employed in various fields including dentistry, where they are present in some types of cements, in endodontic products and, mostly, in dental composite resins [1]. Over the last thirty years these materials have reached a large diffusion throughout the Western world for the treatment of adults and children alike. After performing dental restorations with composite resins, small amounts of uncured molecules are inevitably released into either the oral cavity or – through dentinal diffusion – in pulpal tissues [2–4], hence leaching into the blood [2], a process which may be also facilitated by the mechanical erosion of the material [5].

In some instances, methacrylic monomers display a variable degree of toxicity and may cause, or contribute to, adverse biological effects [6,7] like the damages of the oral soft tissues sometimes observed *in vivo* [1]: it is therefore evident the need of detailed *in vitro* studies regarding the interactions between methacrylates and host [2,3,8]. To understand the reasons of the adverse biological effects, *in vitro* biocompatibility studies of materials containing methacrylates are today performed by multidisciplinary teams including toxicology, biology and chemistry experts. The toxic effects caused by methacrylates are nevertheless still difficult to unravel probably because such molecules can act at different levels [9], for example interfering with the cell cycle and DNA synthesis [10], or increasing the production of reactive oxygen species (ROS) [10,11], or inducing a depletion of intracellular glutathione (GSH) [12]. Such ubiquitous tripeptide is produced in all organs and cells where it accomplishes several physiological tasks including relevant protection against oxidative stress performed through the reduction of hydrogen peroxide and lipid peroxides by converting to its oxidized form (GSSG). The latter is either excreted by the cell or reconverted to GSH by the activity of NADPH-dependent GSH reductase or, alternatively, bound to protein thiol groups forming mixed disulfides [13,14]. GSH can, moreover, also detoxify xenobiotics like methacrylates [15] by conjugating, *via* a Michael addition [16], the thiol group with their α,β-unsaturated carbon–carbon moiety [17] (Patterns 1 and 2). The reaction is catalyzed by glutathione S-transferase (GST), one of several enzyme forms belonging to a multi-gene family – present in cytosol, microsomes and mitochondria – involved in detoxification processes [18–20]. The described reaction, which can also occur in a cell free system [21], deter-

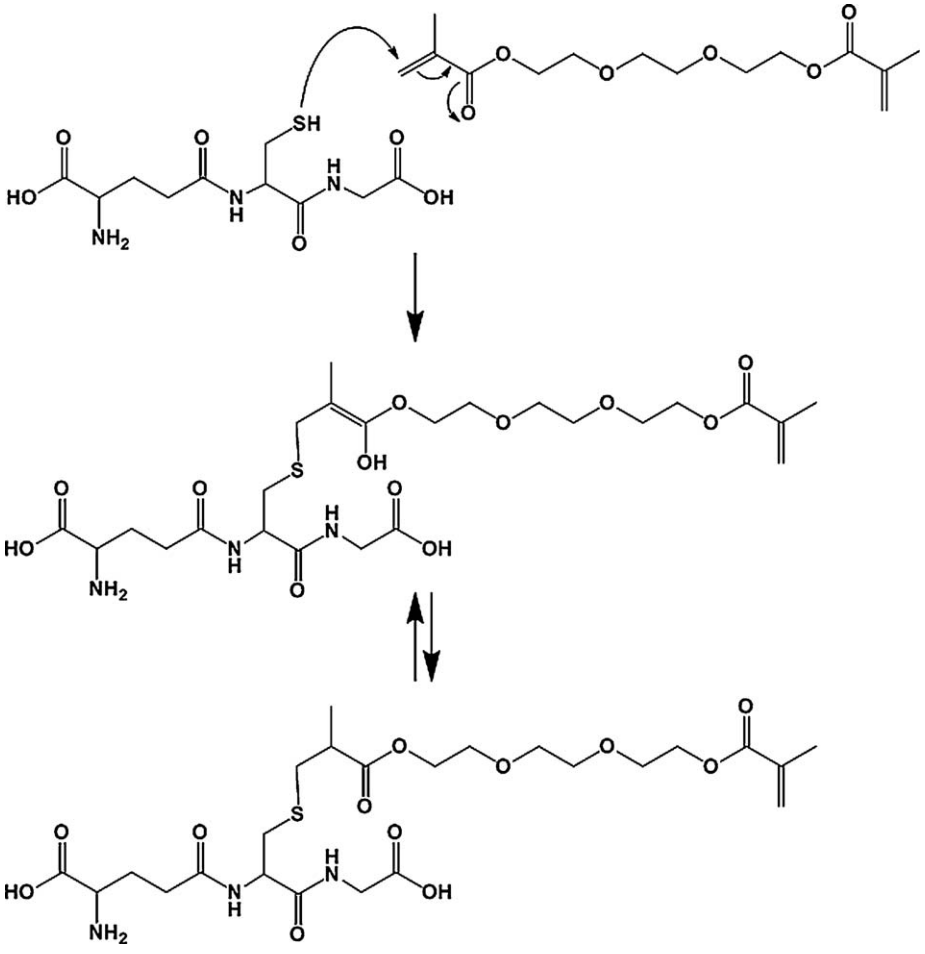

Pattern 1 – Mechanism of the reaction between GSH and TEGDMA: the attack of nucleofilic sulphydrilic group to the terminal carbon of the carbon–carbon double bond causes the π electrons towards oxygen generating the adduct in enolic form; the latter turns out then in equilibrium with the predominant ketonic structure.

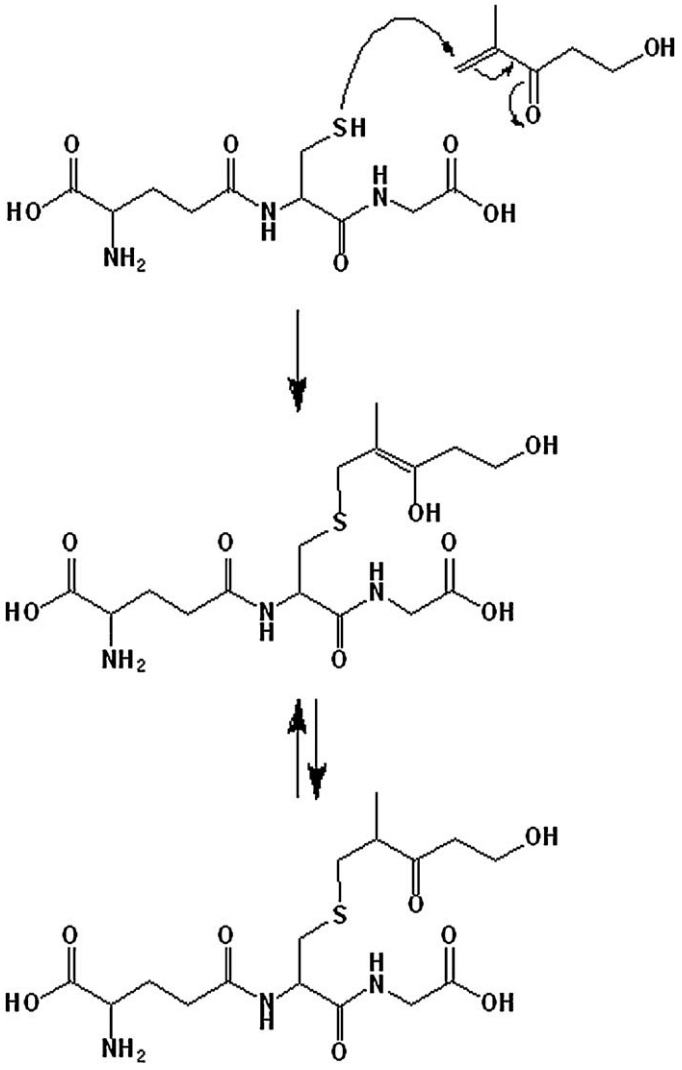

Pattern 2 – Mechanism of the reaction between GSH and HEMA: the attack of nucleofilic sulphydrilic group to the terminal carbon of the carbon–carbon double bond causes the π electrons towards oxygen generating the adduct in enolic form; the latter turns out then in equilibrium with the predominant ketonic structure.

mines GSH cellular depletion [22,23] as observed in several *in vitro* studies employing human fibroblasts [10,17,22,23] and HL-60 cells [24].

The above said process belongs to the metabolism of α,β-unsaturated esters and protects the body against the toxic effects of endo- and xeno-biotic electrophiles. The formation of a bond between the cysteine residue of GSH and an electrophile usually results, in fact, in a less reactive and more water-soluble product [25–27], thus facilitating its clearance from the cells. GSH depletion may have also both positive and negative consequences for the cells: in fact, even if methacrylates removal represents a positive event, the decrease of GSH concentration brings many disadvantages like oxidation of protein thiol groups, protein denaturation and induction of mitochondrial permeability transition [28].

Although the main metabolic pathway for methacrylates detoxification may occur through esterase catalyzed hydrolysis, because only the intact esters are able to overcome the lipophilic barriers [29], methacrylates conjugation with GSH can nevertheless represent a very important alternative route [30]. On the basis of the above considerations, this work aims to set up a method for the detection of the adducts formed by methacrylic monomers with GSH in gingival fibroblasts and erythrocytes using high performance liquid chromatography coupled to mass spectrometry (HPLC–MS) and micellar electrokinetic capillary chromatography (MECK).

Furthermore, molecular docking simulations of HEMA and TEGDMA in the experimental structure of Glutathione S-transferase P1, (the cytosolic enzyme isoform present in gingival fibroblasts) are also reported to rationalize the effectiveness of such enzyme in the catalysis of the reaction of glutathione with methacrylates [17,31].

2. Materials and methods

All chemicals and reagents were supplied by Sigma–Aldrich Srl (Milan, Italy) unless otherwise indicated.

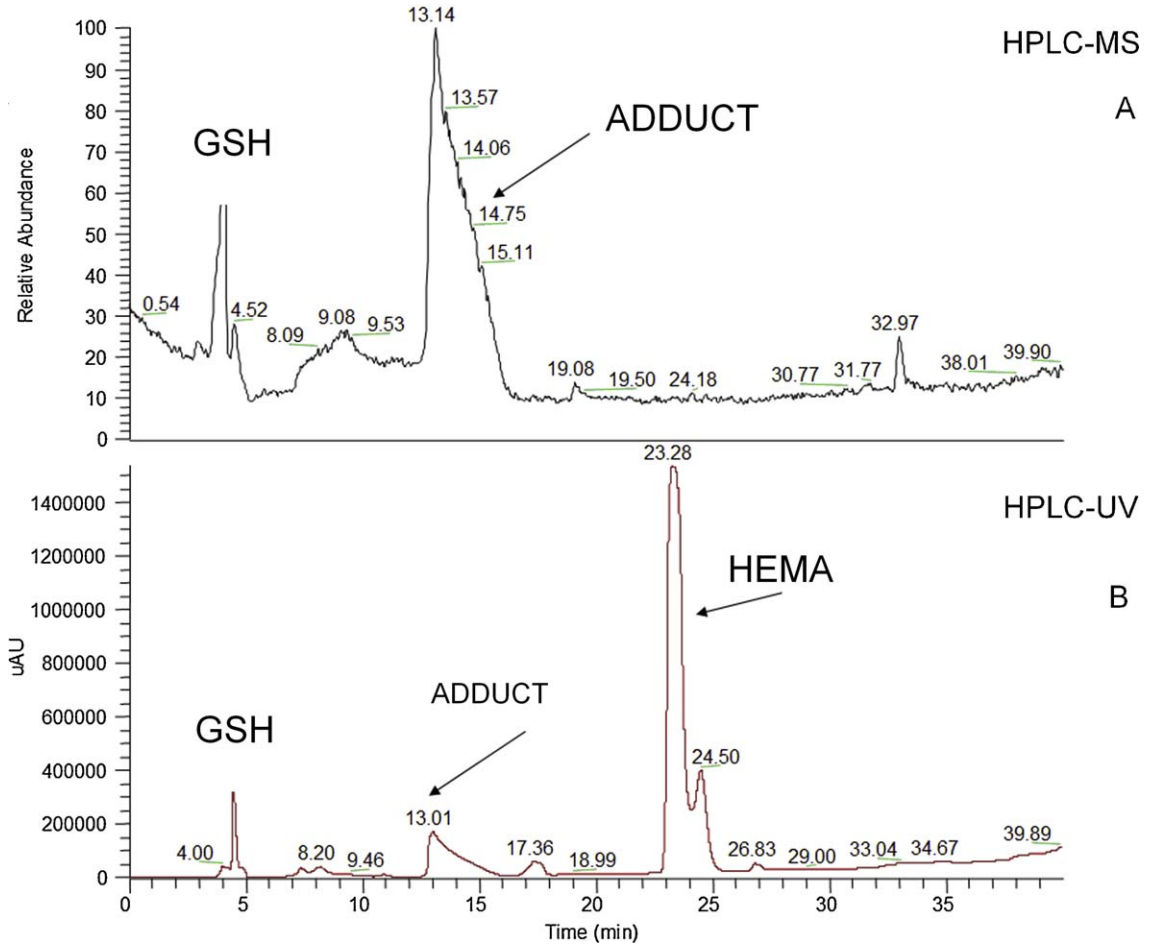

Fig. 1 – Total ion current chromatogram from HPLC–MS analysis (A) and HPLC–UV chromatogram profile (B) of HEMA-GSH mixture after 48 h of incubation.

HPLC grade methanol was purchased from J.T. Baker (Baker Mallinckrodt, Phillipsburg, NJ, USA). HPLC grade water (18.2 mΩ) was prepared using a Millipore Milli-Q purification system (Millipore Corp., Bedford, MA, USA).

2.1. *Synthesis of glutathione-methacrylate adducts*

A solution of GSH (0.8 mmol/L) in phosphate buffer solution (PBS, pH 7.4, 1.0 mL) – bubbled with nitrogen to remove oxygen and inhibit GSH oxidation – was mixed at 37 °C with an equal volume of HEMA (1.0 mmol/L) or TEGDMA (0.4 mmol/L) in PBS [32]; GSH solution in PBS alone was similarly prepared. The reaction mixtures were analyzed immediately and after 48 h by HPLC–MS and MEKC; likewise GSH, HEMA and TEGDMA in PBS solutions were analyzed as controls.

2.2. *Detection of GSH-methacrylate adducts by HPLC–MS and HPLC–UV*

GSH-methacrylate reaction mixtures were analyzed by a SURVEYOR MS micro HPLC, (Thermo Finnigan, San Josè, CA, USA) using a Discovery HS C18 column (250 mm × 4.6 mm, 5 μm) (SUPELCO, Supelco Park, Bellefonte, PA, USA) at a flow rate of 1 mL/min. Water (A) and methanol (B) were used to obtain the chromatographic gradients for the elution: (i) for GSH-TEGDMA reaction mixture, from 5% (B) to 65% (B) in 32 min and then to 95% (B) in 8 min, (ii) for GSH-HEMA reaction mixture, from 25% (B) to 65% (B) in 23 min and then 95% (B) in 7 min followed by 10 min of maintenance. In both cases the column effluent was splitted by a "T junction" positioned after the chromatographic column sharing it between an a UV detector set at 214 nm (80%) and an ESI/MS in positive ion mode (20%) using a Finnigan LCQ DECA XP Max ion trap mass spectrometer equipped with Xcalibur® system manager data acquisition software (Thermo Finnigan, San Josè, CA, USA). The capillary voltage was set at 28 V, the spray voltage was set at 4.8 kV and the tube lens offset was set at 15 V. The capillary temperature was 250 °C. Data were acquired in MS1 scanning mode and recorded in the 50–1500 *m/z* region.

Total ion current (TIC) profile was produced by monitoring, during the chromatographic run, the intensity of all the ions produced and acquired in every scan.

2.3. *Detection of GSH-methacrylate adducts by MEKC*

To obtain the electrophoretic profiles of HEMA, TEGDMA, GSH and reaction mixtures, a capillary electrophoresis system (P/ACE^{TM} MDQ, Beckman, Richmond, CA USA) with a fused sil-

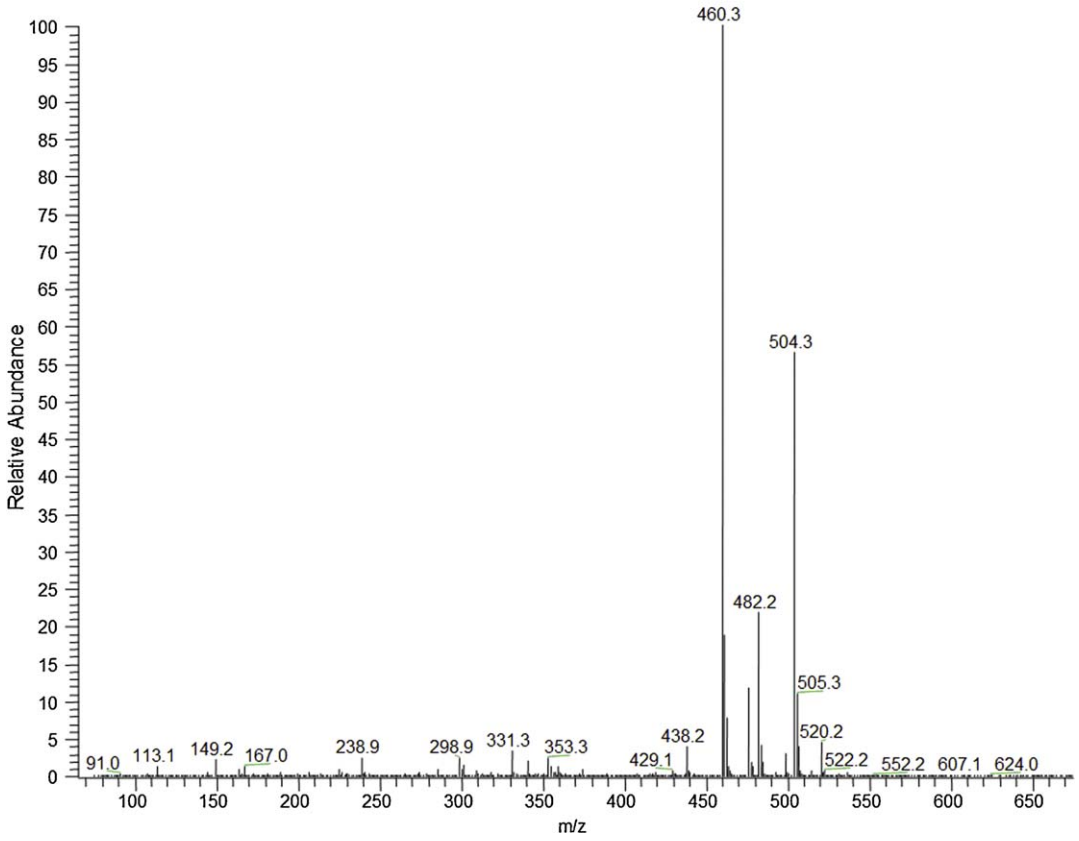

Fig. 2 – HPLC–MS analysis of HEMA-GSH mixture after 48 h of incubation: MS spectrum of the peak eluted at t_R 13.14 min. The peak at *m/z* 438 in the mass spectrum is originated by the GSH-HEMA adduct. Signals corresponding to sodium adducts are also present in the spectrum at *m/z* = 460 $[M + Na]^+$, 482 $[M + 2Na - H]^+$, 504 $[M + 3Na - 2H]^+$.

ica capillary (60 cm length, 50 μm inner ∅, Beckman) was used; a 0.2 mm detection window was obtained by a small flame at 10 cm from the cathodic terminal. The running solution was constituted by sodium phosphate/sodium tetraborate buffer (44.4 and 11.1 mmol/L, respectively), pH 7.19, with 36.7 mmol/L SDS as micellar phase and a final content of acetonitrile (10%, v/v). Samples were diluted (1:1) with a solution of sodium phosphate (7.2 mmol/L) and sodium tetraborate (1.8 mmol/L) at pH 7.19 and injected by pressure (0.5 psi) for 10 s at the anodic end of the capillary. After every run the capillary was washed (20 psi) with H_2O, H_2O/acetonitrile 1:1, H_2O, NaOH and finally H_2O. Each analysis was performed at a constant voltage of 18 kV with a current of nearly 50 μA at a temperature of 35 °C and at a wavelength of 214 nm. The adducts previously isolated and identified by HPLC–MS were also analyzed in the same operative conditions.

2.4. *Treatment of red blood cells with methacrylates and detection of the formed adducts*

Red blood cell suspensions (1.0 mL, 5% final hematocrit) were incubated in a shaking water bath for 1 h at 37 °C with HEMA (4 mmol/L) or TEGDMA (2 mmol/L) in PBS. As controls, red blood cell suspensions (1.0 mL, 5% hematocrit) in absence of monomers were used. After incubation, the samples were centrifuged (500 × *g*, 5 min), the precipitated cells were lysed by freezing and proteins were eliminated by precipitation with metaphosphoric acid (5% m/v) and following centrifugation at 15000 × *g* (10′, 4 °C); the samples were then analyzed by MEKC. The diluted extracellular media (filtered by a 45 μm millipore filter) were also analyzed by MEKC.

2.5. *Cell culture of human gingival fibroblasts*

Human gingival fibroblasts were obtained (with informed consent) from a healthy patient subjected to gingivectomy of the molar region. Immediately after removal, the tissues were placed in Hanks' Balanced Salt Solution (HBSS) with penicillin (250 U/mL), streptomycin (0.25 mg/mL), gentamycin (0.05 mg/mL), and amphothericin B (0.0025 mg/mL). The epithelial layer was detached mechanically and the subepithelial specimens were plated in tissue culture flasks with Dulbecco's Modification of Eagles' Medium (DMEM), supplemented with 50% fetal calf serum (FCS), L-glutamine (2 mM), sodium pyruvate (1 mM), penicillin (50 UI/mL) and streptomycin (50 μg/mL), at 37 °C in a 5% humidified CO_2 atmosphere. After the first passage, the gingival fibroblasts were routinely cultured in DMEM supplemented with 10% FCS [33,34] and were not used beyond the fifth passage [35].

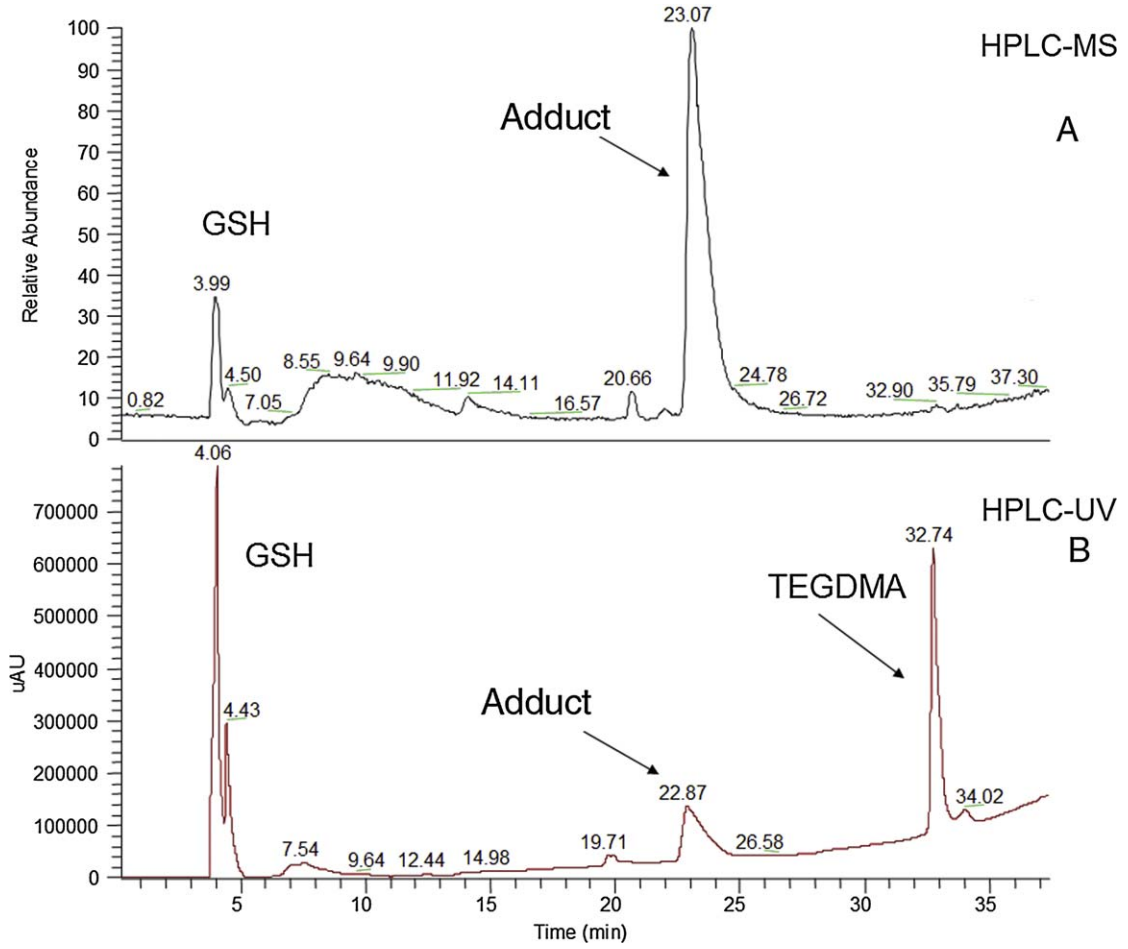

Fig. 3 – Total ion current chromatogram from HPLC–MS analysis (A) and HPLC–UV chromatogram profile (B) of TEGDMA-GSH mixture after 48 h of incubation.

2.6. *Treatment of human primary fibroblasts with methacrylates and detection of the formed adducts*

Cells were plated in 6-wells plates at a density of approximately 25,000 cells/cm^2 and cultured to subconfluent monolayer; HEMA (4 mmol/L) or TEGDMA (2 mmol/L) in PBS were then added and the cells were incubated for 1 h at 37 °C. Cell monolayers without monomers were used as controls. After incubation, the cells were lysed by freezing, and proteins were eliminated by precipitation with metaphosphoric acid (5% m/vol) and following centrifugation at 14,500 g (10 min, 4 °C); the samples were then analyzed by MEKC. The extracellular media (filtered by a 45 μm millipore filter) were also analyzed by MEKC.

2.7. *Molecular modeling*

All calculations were performed on a PC cluster using AMD 64 bit CPUs and running the Debian Linux operating system.

2.7.1. *GST structure preparation*

Two three-dimensional (3-D) GST co-crystallized with etacrinic acid (EAA) in two different bound conformations were retrieved from the PDB (http://www.pdb.org/) [36] archive (pdb entry codes: 11gs [31] and 3gss [37], Fig. 11). The co-crystals containing the etacrinic acid compounds were chosen for the structural similarities with the molecules under studies, i.e. TEGDMA and HEMA. The structures were refined by AMBER 8.0 [38] program using the following protocol. AM1-BCC charges were calculated on the glutathione/etacrinic acid adduct employing the Amber antechamber module. Using the xLeap Amber module, the starting complexes were added of the hydrogen atoms and solvated in a octahedral box of TIP3P water with each box side at least 10.0 Å away from the nearest atoms of the complexes. Proper ions were included to neutralize the charge of the system. The ions were placed randomly in the system 10 Å away from the nearest atoms. The hydrogen atoms, counter ions and water molecules were then minimized for 1000 iterations. Then the whole complexes were relaxed for 5000 iterations. The Amber-all-atom (parm99) and the GAFF force fields were used in all calculations.

2.7.2. *Docking procedure*

The docking studies were performed using Autodock 4.0 [39]. The two GTS complexes were aligned by means of

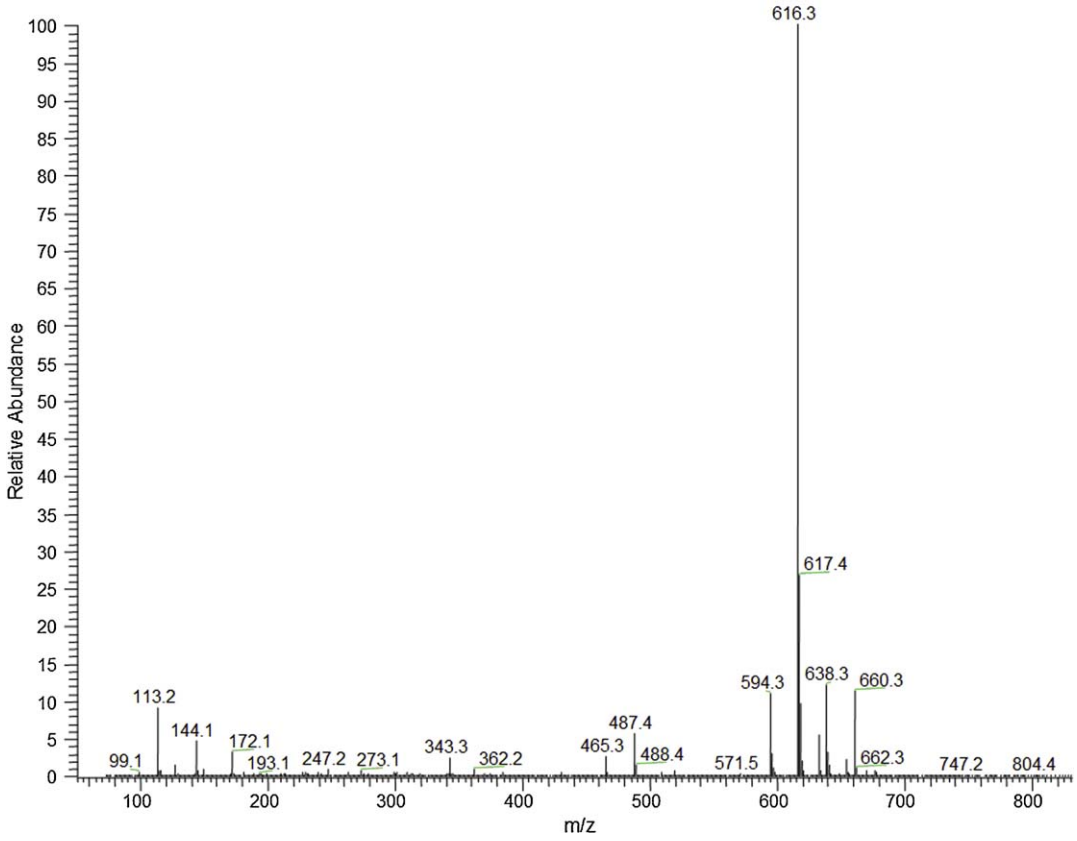

Fig. 4 – HPLC–MS analysis of TEGDMA-GSH mixture after 48 h of incubation: MS spectrum of the peak eluted at t_R 23.07 min. The peak at *m/z* 594 in the mass spectrum is due to an adduct formed between one molecule of GSH and one molecule of TEGDMA. Peaks at *m/z* 616, 638 and 660, correspond to the adducts with one, two and three molecules of sodium respectively.

UCSF Chimera MatchMaker tool [40]. The molecule structures of TEGDMA and HEMA were built using the cdk libraries through a java implementation available on the RCMD website (http://www.rcmd.it). The Autodock graphical interface AutoDock Tools package 1.5.0 was employed to generate the docking input files and to analyze the docking results; the same procedure as described in the manual was followed. A grid box size of $50 \times 50 \times 50$ points spacing of 0.375 Å were used, centered to the bound etacrinic acids and covered most of the catalytic pocket of both enzymes. For all the inhibitors, the single bonds excluding the amide bonds were treated as active torsional bonds. One hundred structures, i.e. 100 runs, were generated using Lamarckian genetic algorithm. A default protocol was applied, with an initial population of 150 randomly placed individuals, a maximum number of 2.5×10^6 energy evaluations, and a maximum number of 2.7×10^4 generations. A mutation rate of 0.02 and a crossover rate of 0.8 were used. The 100 poses obtained in each GSH were joined and clustered with a root mean square deviation (RMSD) value of 2.0. To validate the docking method, a random EAA conformation was generated and docked into either 11gs or 3gss proteins deprived of the co-crystallized EAA. Autodock proved to reposition the modeled EAA with RMSD errors lower than 2.0 (data not shown).

3. Results

3.1. *HPLC–MS and HPLC–UV analysis of GSH-methacrylate adducts*

The total ion current (Panel A) and the HPLC–UV (Panel B) chromatograms obtained from the analysis of GSH-HEMA adduct are shown in Fig. 1 In particular, in the HPLC–MS profile, the compound eluted at t_R of 13.14 min gave rise to a peak at *m/z* 438 in the mass spectrum, corresponding to that of an adduct formed between one molecule of GSH and one molecule of HEMA (Fig. 2). Signals corresponding to several sodium adducts were also present in the spectrum: $[M + Na]^+$ at *m/z* = 460, $[M + 2Na - H]^+$ at *m/z* = 482 and $[M + 3Na - 2H]^+$ at *m/z* = 504.

In Fig. 3 the total ion current (Panel A) and the HPLC–UV (Panel B) chromatograms relative to the analysis of GSH-TEGDMA adduct are showed. Also in this case, was present in the HPLC/ESI-ITMS profile a peak relative to the adduct formation between one molecule of GSH and one molecule of TEGDMA (t_R 23.07 min). The peak arising at *m/z* 594 in the mass spectrum, corresponding to the protonated molecular ion, and peaks at *m/z* 616, 638 and 660, due to adducts with one, two and

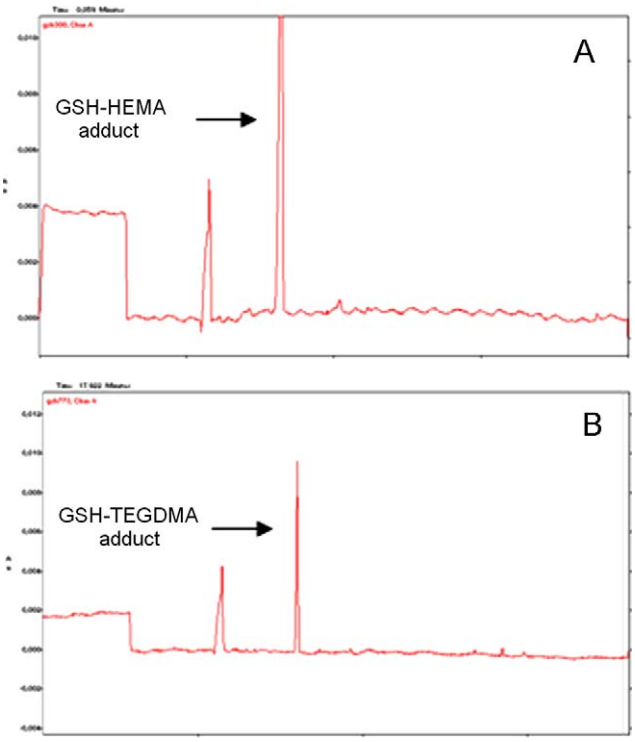

Fig. 5 – (A) Electrophoretic separation of GSH-HEMA adduct, after isolation in HPLC. The signal of this molecule appears at 8.5 min of the running time. (B). Electrophoretic separation of GSH-TEGDMA adduct, after isolation in HPLC. The signal of this molecule appears at 8.0 min of the running time

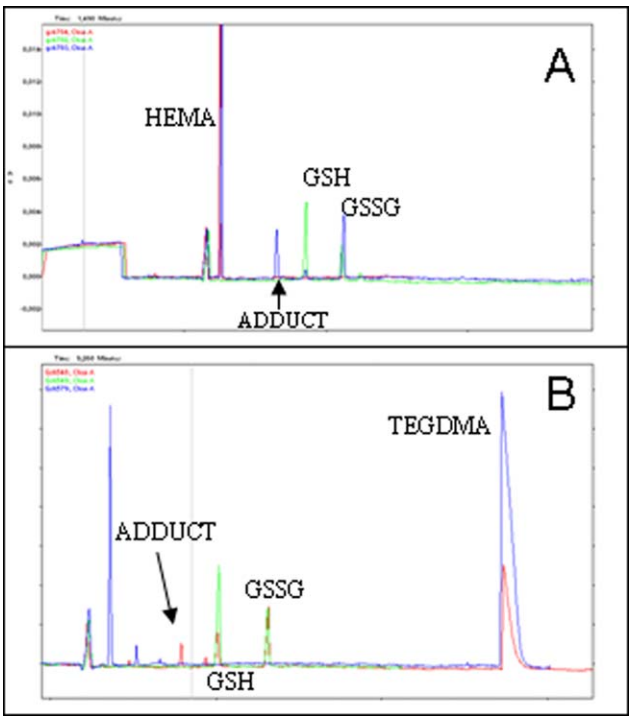

Fig. 6 – (A) MEKC separation of mixture reaction between GSH and HEMA, it is possible to see the signal corresponding to GSH, GSSG, HEMA and a signal with the same running time of adduct. (B) MEKC separation of mixture reaction between GSH and TEGDMA, it is possible to see the signal corresponding to GSH, GSSG, TEGDMA and a signal with the same running time of adduct.

three sodium ions respectively (Fig. 4), confirmed the structure of the adduct.

3.2. *MEKC analysis of GSH-methacrylate adducts*

GSH, HEMA and TEGDMA were analyzed by MEKC obtaining their electrophoretic runs; then a similar analysis was carried out with the samples collected from HPLC–MS containing the isolated adducts. In this way the electrophoretic rate time of the GSH-methacrylate adducts was obtained (Fig. 5A and B). Finally the reaction mixture of GSH and HEMA (Fig. 6A) was analyzed and the electropherograms clearly showed the presence of signals corresponding to the reagents (GSH, GSSG, HEMA) plus a peak at the same retention time as the previously examined GSH-HEMA adduct. This same procedure was repeated for the reaction mixture of GSH and TEGDMA and also this electrophoretic profile showed a signal at the same retention time previously recorded for the GSH -TEGDMA adduct (Fig. 6B). The described signals were not present in the control samples.

3.3. *Detection by MEKC of the methacrylate-GSH adducts produced in cells*

In the electropherograms of control erythrocytes lysates, the GSH and GSSG signals were identified (Fig. 7A), whereas after incubation with HEMA or TEGDMA also the signals of monomers and adducts, the latter of low intensity, were identified, (Fig. 8 Figs. 7A and 8A respectively). In the electropherograms of extracellular medium, the signals of both monomers and adducts, the latter higher than in the intracellular fluids, were observed (Figs. 7B and 8B).

As for the reaction HEMA-GSH in human gingival fibroblasts is regarded, the following results were obtained: the signal of GSH was normally present in the intracellular portion of fibroblasts not treated with methacrylate monomers (Fig. 9A). In the intracellular sample, incubated for 1 h with HEMA 4 mmol/L, in addition to the signal of HEMA and GSH, a signal that corresponds to a substance with the same migration time of GSH-HEMA adduct was found (Fig. 9A).

Subsequently, the extracellular portion of fibroblasts incubated with HEMA was analyzed in MEKC showing a signal corresponding to HEMA-GSH adduct, unlike the untreated sample (Fig. 9B). Also the fibroblasts incubated with TEGDMA displayed, in the electropherograms, a peak corresponding to adduct peak (absent in the control) both in intracellular (Fig. 10A) and in extracellular (Fig. 10B) portions.

3.4. *Molecular modeling*

Docking calculations were performed to investigate the interactions that lead to the formation of either the TEGDMA-GSH or the HEMA-GSH complexes. The EAA-GSH complexes

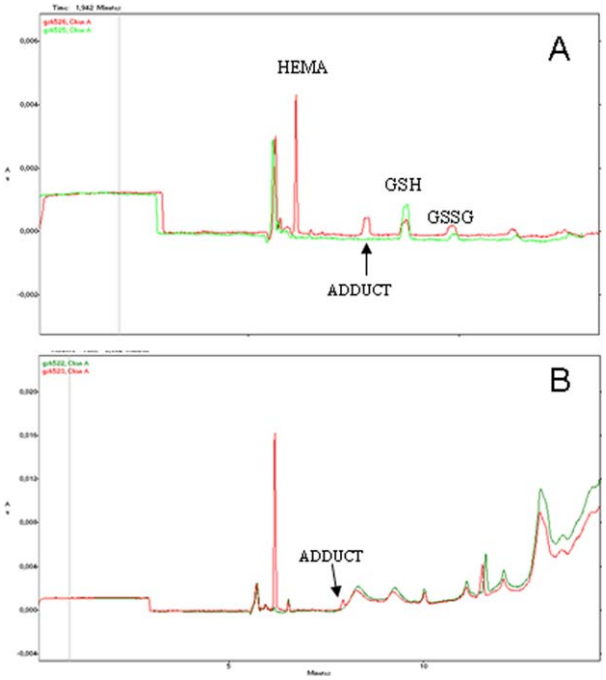

Fig. 7 – Electrophoretic profiles of erythrocytes intracellular medium (A) and of erythrocytes extracellular fluid (B) obtained after 1 h of incubation in presence (red) or in absence (green) of HEMA. (For interpretation of references to color in this figure legend, the reader is referred to the web version of this article.)

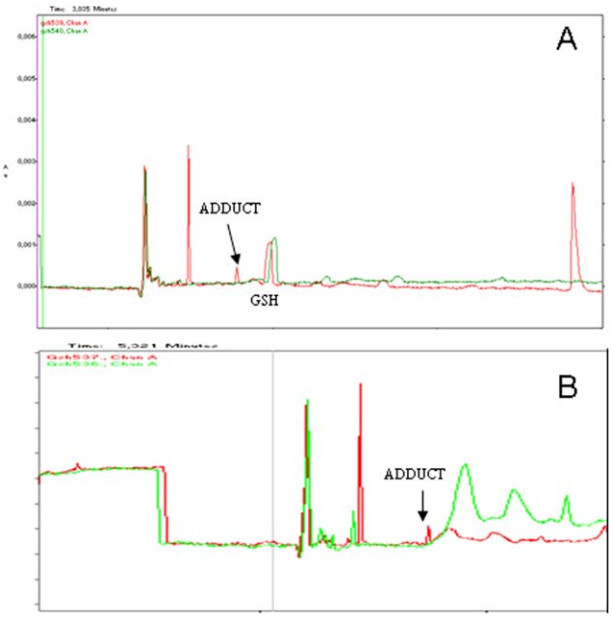

Fig. 8 – Electrophoretic profiles of erythrocytes intracellular fluid (A) and erythrocytes extracellular medium (B) obtained after 1 h of incubation in presence (red) or in absence (green) of TEGDMA. (For interpretation of references to color in this figure legend, the reader is referred to the web version of this article.)

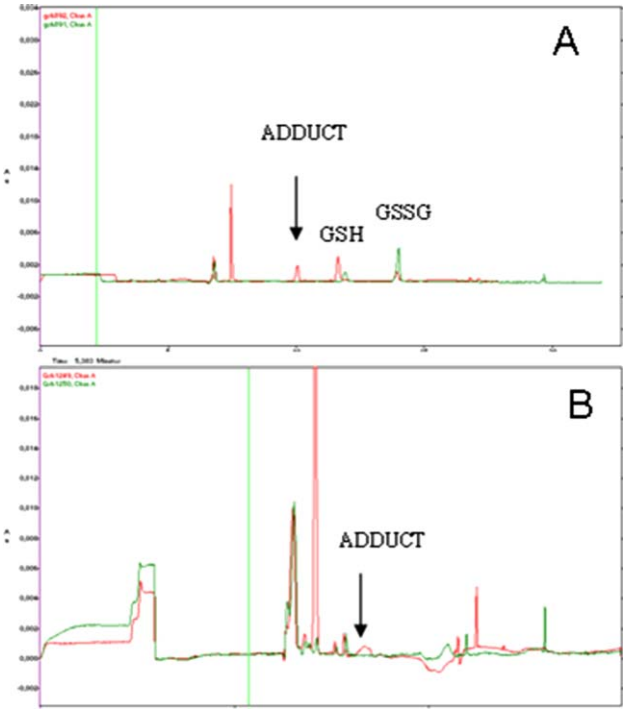

Fig. 9 – Electrophoretic profiles of gingival fibroblasts intracellular fluid (A) and gingival fibroblasts extracellular medium (B) obtained after 1 h of incubation in presence (red) or in absence (green) of HEMA. (For interpretation of references to color in this figure legend, the reader is referred to the web version of this article.)

(Fig. 11) were chosen due to the structure similarities of EEA with TEGDMA and HEMA, assuming a similar mechanism for adduct formation. Two different etacrinic bound conformations also allowed the inclusion in the docking calculations of some conformational variability in the receptor site (cross-docking). The conformation associated with the lowest docking energy of the most populated cluster for each cross-docking was then used to define the pre-covalent TEGDMA-GSH or the HEMA-GSH complexes.

Analysis of either TEGDMA or HEMA docked conformations (Figs. 12 and 13) highlighted that the two monomers are indeed able to recognize the binding pocket and to place the double bonds sp^2 carbon atoms at a reactive distances ($C_{HEMA}\ldots S_{Glutathione} = 3.55$ Å; $C_{TEGDMA}\ldots S_{Glutathione} = 3.19$ Å) from the cysteine thiol to promote the Michael reaction.

Since GSH is highly conserved in all the different cellular lines, we can assume that the formation of the adduct occurs with the same chemical recognition pathway in any tissue and thus also for both the erythrocyte and gingival fibroblast enzymes.

4. Discussion

In this paper we present a method to detect and identify, either in presence and in absence of cells, GSH-methacrylate adducts obtained *via* a Michael addition reaction, catalyzed – only in cellular system – by GST enzymes. The approach herein pre-

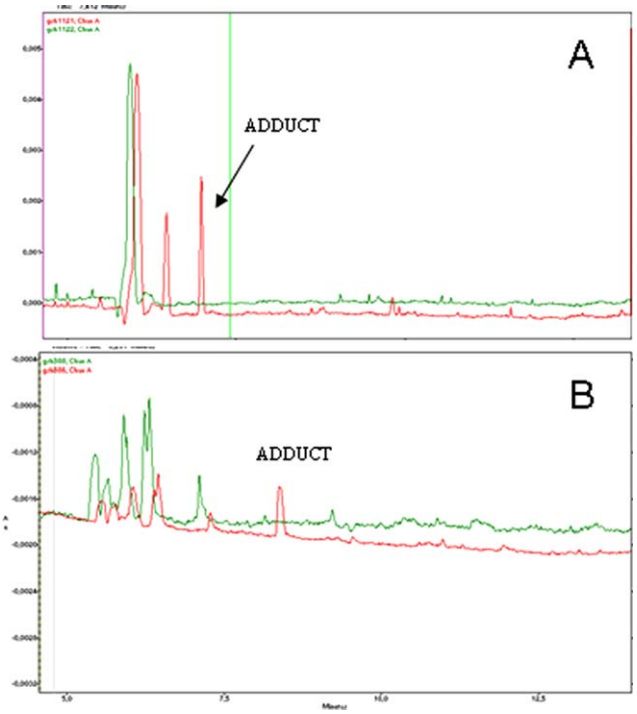

Fig. 10 – Electrophoretic profiles of gingival fibroblasts intracellular fluid (A) and gingival fibroblasts extracellular medium (B) obtained after 1 h of incubation in presence (red) or in absence (green) of TEGDMA. (For interpretation of references to color in this figure legend, the reader is referred to the web version of this article.)

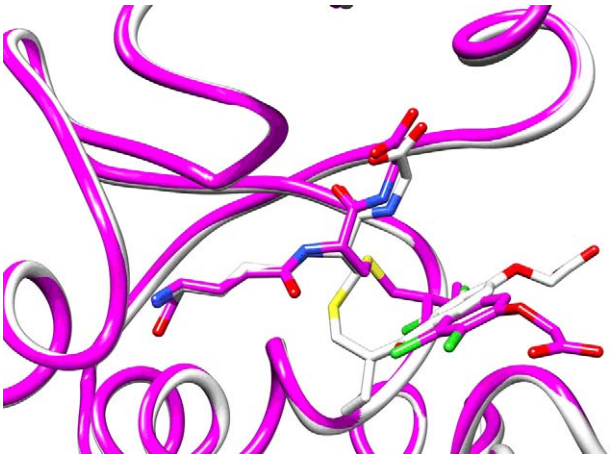

Fig. 11 – Superimposition of the 11gs (white) and 3gss (magenta) GST/GSH/EAA complexes. Note the different bound conformations of the GSH/EAA adducts. In ribbon are reported the GST protein structures superimposed and in stick the glutathione-EAA adducts. (For interpretation of references to color in this figure legend, the reader is referred to the web version of this article.)

sented, based on HPLC–MS and MEKC analytical techniques, is sensitive and endowed with high resolution.

The HPLC–MS analytical conditions were optimized according to the physico-chemical properties of HEMA, TEGDMA and GSH allowing their successful separation in a PBS solution. Subsequently, the analysis of the reaction mixtures containing HEMA or TEGDMA and GSH revealed the presence of compounds which (by mass spectra examination) were identified as the HEMA-GSH and TEGDMA-GSH adducts, respectively.

By the way, the operating conditions utilized for the HPLC–MS analysis of the reaction mixtures in PBS were not suitable for examining the adducts present inside and outside the cells because of several interfering signals due to the components of culture medium. By MECK analysis was however obtained a successful separation ascribable to the presence – in the running buffer – of a micellar phase which introduces an additional separation mechanism and a solubilisation effect in presence of biological materials. The adducts, collected after HPLC isolation, were used as standards for MECK (see again Figs. 5A and 5B).

The formation of the adducts shows different kinetics when the reaction occurs in PBS medium (24–48 h) or in cells

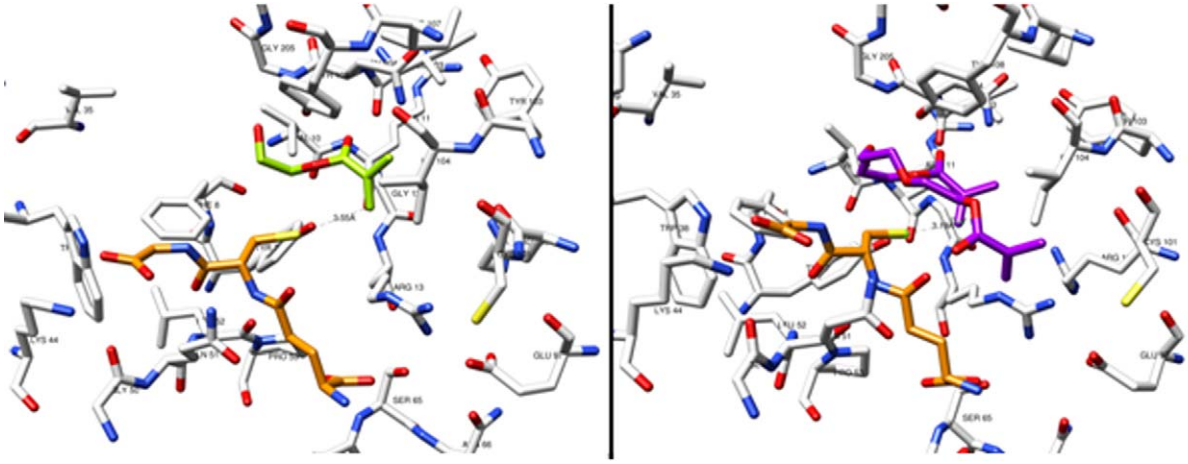

Fig. 12 – Autodock proposed bound conformation of HEMA (left, green colored carbon atoms) and TEGDMA (right, purple colored carbon atoms). GST carbon atoms are reported in white and glutathione carbon atoms are in orange. (For interpretation of references to color in this figure legend, the reader is referred to the web version of this article.)

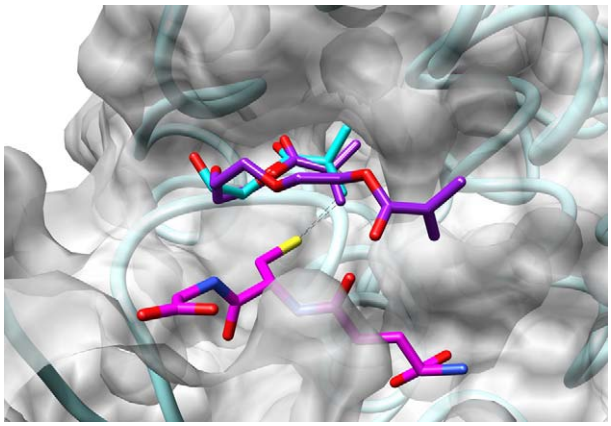

Fig. 13 – Superimoposed docked conformations of TEGDMA (stick purple colored carbon atoms) and HEMA (stick cyan colored carbon atoms) into GST/GSH complex. In stick is also reported the glutathione (magenta colored carbon atoms). The van der Waals surface of GST is also represented. (For interpretation of references to color in this figure legend, the reader is referred to the web version of this article.)

(1 h, both in gingival fibroblasts and in erythrocytes) probably due to the presence of GST enzymes, as suggested by previous studies [18–20] and inferred from the molecular modeling results here reported. The latter studies showed that the putative groups involved in the adduct formation are at a covalent-bond-compatible distance between the GSH sulfur atom and the methylene sp^2 carbon atom of methacrylates (Fig. 12).

As well known, the formed adducts are cleared from the cells (as here also observed) to be metabolized and converted to mercapturic acids: in such form they are then delivered to the kidney for excretion in urine or involved in further metabolism [29].

Methacrylates may also undergo a different pathway: in fact they can be converted – by unspecific esterases present in saliva or blood – to methacrylic acid, a physiological substrate of the valine pathway, which is lastly metabolized to CO_2 *via* methylmalonyl-CoA and succinyl-CoA in Krebs cycle [28,41,42].

5. Conclusions

The described analytical method allowed the *in vitro* identification of GSH-methacrylate adducts; since such compounds undergo, as previously reported, further transformations, their detection also in body fluids imply the deep knowledge of the kinetic of the metabolic processes; nevertheless the high sensitivity of the employed method could not bar such possibility in the not too distant future.

Acknowledgements

The authors acknowledge Dr. Luca Romanelli, Sapienza University of Rome, for critically reading the manuscript.

REFERENCES

[1] Geurtsen W. Biocompatibility of resin-modified filling materials. Crit Rev Oral Biol Med 2000;11(3):333–55.
[2] Bouillaguet S, Wataha JC, Hanks CT, Ciucchi B, Holz J. In vitro cytotoxicity and dentin permeability of HEMA. J Endod 1996;22(5):244–8.
[3] Bouillaguet S, Virgillito M, Wataha J, Ciucchi B, Holz J. The influence of dentine permeability on cytotoxicity of four dentine bonding systems, in vitro. J Oral Rehabil 1998;25(1):45–51.
[4] Gerzina TM, Hume WR. Diffusion of monomers from bonding resin–resin composite combinations through dentine in vitro. J Dent 1996;24(1–2):125–8.
[5] Ortengren U. On composite resin materials. Degradation, erosion and possible adverse effects in dentists. Swed Dent J Suppl 2000;141:1–61.
[6] Geurtsen W, Lehmann F, Spahl W, Leyhausen G. Cytotoxicity of 35 dental resin composite monomers/additives in permanent 3T3 and three human primary fibroblast cultures. J Biomed Mater Res 1998;41(3):474–80.
[7] Geurtsen W, Spahl W, Leyhausen G. Residual monomer/additive release and variability in cytotoxicity of light-curing glass-ionomer cements and compomers. J Dent Res 1998;77(12):2012–9.
[8] Goldberg M. In vitro and in vivo studies on the toxicity of dental resin components: a review. Clin Oral Investig 2008;12(1):1–8.
[9] Schweikl H, Spagnuolo G, Schmalz G. Genetic and cellular toxicology of dental resin monomers. J Dent Res 2006;85(10):870–7.
[10] Chang HH, Guo MK, Kasten FH, Chang MC, Huang GF, Wang YL, et al. Stimulation of glutathione depletion ROS production and cell cycle arrest of dental pulp cells and gingival epithelial cells by HEMA. Biomaterials 2005;26(7):745–53.
[11] Spagnuolo G, D'Anto V, Cosentino C, Schmalz G, Schweikl H, Rengo S. Effect of N-acetyl-L-cysteine on ROS production and cell death caused by HEMA in human primary gingival fibroblasts. Biomaterials 2006;27:1803–9.
[12] Volk J, Engelmann J, Leyhausen G, Geurtsen W. Effects of three resin monomers on the cellular glutathione concentration of cultured human gingival fibroblasts. Dent Mater 2006;22:499–505.
[13] Forman HJ, Shi MM, Iwamoto T, Liu RM, Robison TW. Measurement of gamma-glutamyl transpeptidase and gamma-glutamylcysteine synthetase activities in cells. Methods Enzymol 1995;252:66–71.
[14] Toroser D, Yarian CS, Orr WC, Sohal RS. Mechanisms of gamma-glutamylcysteine ligase regulation. Biochim Biophys Acta 2006;1760(2):233–44.
[15] Boyland E, Chasseaud LF. Enzyme-catalysed conjugations of glutathione with unsaturated compounds. Biochem J 1967;104(1):95–102.
[16] Michael A. Ueber die Addition von Natriumacetessig- und Natriummalonsäureäthern zu den Aethern ungesättigter Säuren. Journal für Praktische Chemie 1887;35(1):349–56.
[17] Lefeuvre M, Bourd K, Loriot MA, Goldberg M, Beaune P, Perianin A, et al. TEGDMA modulates glutathione transferase P1 activity in gingival fibroblasts. J Dent Res 2004;83(12):914–9.
[18] Ghanayem BI, Burka LT, Matthews HB. Ethyl acrylate distribution, macromolecular binding, excretion, and metabolism in male Fisher 344 rats. Fundam Appl Toxicol 1987;9(3):389–97.
[19] Potter DW, Tran TB. Rates of ethyl acrylate binding to glutathione and protein. Toxicol Lett 1992;62(2–3):275–85.

[20] Freidig A, Hofhuis M, van Holstijn I, Hermens J. Glutathione depletion in rat hepatocytes: a mixture toxicity study with α,β-unsaturated esters. Xenobiotica 2001;31(5):295–307.
[21] Schults TW, Yarbrough JW, Hunter RS, Aptula AO. Verification of the structural alerts for Michael acceptors. Chem Res Toxicol 2007;20:1359–63.
[22] Engelmann J, Leyhausen G, Leibfritz D, Geurtsen W. Effect of TEGDMA on the intracellular glutathione concentration of human gingival fibroblasts. J Biomed Mater Res 2002;63(6):746–51.
[23] Stanislawski L, Lefeuvre M, Bourd K, Soheili-Majd E, Goldberg M, Perianin A. TEGDMA-induced toxicity in human fibroblasts is associated with early and drastic glutathione depletion with subsequent production of oxygen reactive species. J Biomed Mater Res A 2003;66(3):476–82.
[24] Nocca FG, De Palma F, Minucci A, De Sole P, Martorana GE, Calla C, et al. Alterations of energy metabolism and glutathione levels of HL-60 cells induced by methacrylates present in composite resins. J Dent 2007;35(3):187–94.
[25] Alin P, Mannervik B, Jornvall H. Structural evidence for three different types of glutathione transferase in human tissues. FEBS Lett 1985;182(2):319–22.
[26] Tjalkens RB, Luckey SW, Kroll DJ, Petersen DR. Alpha, beta-unsaturated aldehydes increase glutathione S-transferase mRNA and protein: correlation with activation of the antioxidant response element. Arch Biochem Biophys 1998;359(1):42–50.
[27] Eaton DL, Bammler TK. Concise review of the glutathione S-transferases and their significance to toxicology. Toxicol Sci 1999;49:146–64.
[28] Freeman ML, Huntley SA, Meredith MJ, Senisterra GA, Lepock J. Destabilization and denaturation of cellular protein by glutathione depletion. Cell Stress Chaperones 1997;2(3):191–8.
[29] Greim H, Ahlers J, Bias R, Broecker B, Hollander H, Gelbke HP, et al. Assessment of structurally related chemicals: toxicity and ecotoxicity of acrylic acid and acrylic acid alkyl esters (acrylates), methacrylic acid and methacrylicacid alkyl esters (methacrylates). Chemosphere 1995;31:2637–59.
[30] Hinchman CA, Ballatori N. Glutathione conjugation and conversion to mercapturic acids can occur as an intrahepatic process. J Toxicol Environ Health 1994;41(4):387–409.
[31] Oakley AJ, LoBello M, Mazzetti AP, Federici G, Parker MW. The glutathione conjugate of ethacrynic acid can bind to human pi class glutathione transferase P1-1 in two different modes. FEBS Lett 1997;419(1):32–6.
[32] McCarthy TJ, Hayes EP, Schwartz CS, Witz G. The reactivity of selected acrylate esters toward glutathione and deoxyribonucleosides in vitro: structure–activity relationships. Fundam Appl Toxicol 1994;22(4):543–8.
[33] Quaglino D, Boraldi F, Barbieri D, Croce A, Tiozzo R, Pasquali Ronchetti I. Abnormal phenotype of in vitro dermal fibroblasts from patients with pseudoxanthoma elasticum (PXE). Biochim Biophys Acta 2000;1501(1):51–62.
[34] Tiozzo Costa R, Baccarani Contri M, Cingi MR, Pasquali Ronchetti I, Salvini R, Rindi S, et al. Pseudoxanthoma elasticum (PXE): ultrastructural and biochemical study on proteoglycan and proteoglycan-associated material produced by skin fibroblasts in vitro. Coll Relat Res 1988;8(1):49–64.
[35] Scotti R, Tiozzo R, Parisi C, Croce MA, Baldissara P. Biocompatibility of various root canal filling materials ex vivo. Int Endod J 2008;41(8):651–7.
[36] Bernstein FC, Koetzle TF, Williams GJ, Meyer Jr EF, Brice MD, Rodgers JR, et al. The protein data bank: a computer-based archival file for macromolecular structures. J Mol Biol 1977;112(3):535–42.
[37] Oakley AJ, Rossjohn J, LoBello M, Caccuri AM, Federici G, Parker MW. The three-dimensional structure of the human Pi class glutathione transferase P1-1 in complex with the inhibitor ethacrynic acid and its glutathione conjugate. Biochemistry 1997;36(3):576–85.
[38] Ponder JW, Case DA. Force fields for protein simulations. Adv Protein Chem 2003;66:27–85.
[39] Morris GM, Huey R, Olson AJ. Using AutoDock for ligand-receptor docking. Curr Protoc Bioinformatics 2008. Chapter 8 (Unit 8–14).
[40] Pettersen EF, Goddard TD, Huang CC, Couch GS, Greenblatt DM, Meng EC, et al. UCSF Chimera – a visualization system for exploratory research and analysis. J Comput Chem 2004;25(13):1605–12.
[41] Durner J, Kreppel H, Zaspel J, Schweikl H, Hickel R, Reichl FX. The toxicokinetics and distribution of 2-hydroxyethyl methacrylate in mice. Biomaterials 2009;30: 2066–71.
[42] Seiss M, Marquardt W, Hickel R, Reichl FX. Excretion of dental resin monomers and metabolic intermediates via urine in guinea pigs. Dental Mater 2009;25:481–5.